Electronic Supplementary Information

Solvent and Stoichiometry-dependent Versatile Organogelation and Robust Crystallization from Supramolecular Association of Adipic Acid and Triethanolamine

Gerald Lepcha,[a] Indrajit Pal,[a] Santanu Majumadar,[a] Yogesh Dhasmana,[b] Sanjay Mondal,[c] Ennio Zangrando,[d] Deepak Chopra,[b,*] and Biswajit Dey[a,*]

[a]Department of Chemistry, Visva-Bharati University, Santiniketan-731235, India

E-mail: bdeychem@gmail.com, biswajit.dey@visva-bharati.ac.in (B.D.)

[b]Department of Chemistry, IISER Bhopal, Bhopal Bypass Road, Bhauri, Bhopal 462066

E-mail: dchopra@iiserb.ac.in (D. C.)

[c]Department of Chemistry, The University of Burdwan, Burdwan, India

[d]Department of Chemical and Pharmaceutical Sciences, University of Trieste, 34127 Trieste, Italy

1. EDS elemental analyses.

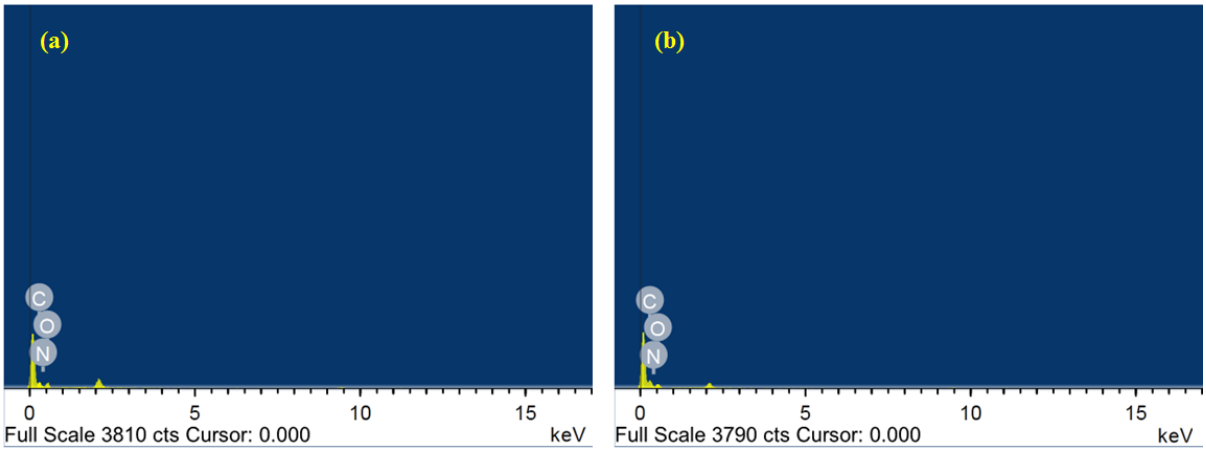

Fig. S1. EDAX elemental spectrum of (a) **ADP-TEA-DMF**, and (b) **ADP-TEA-DMF-MeCN** organogels.

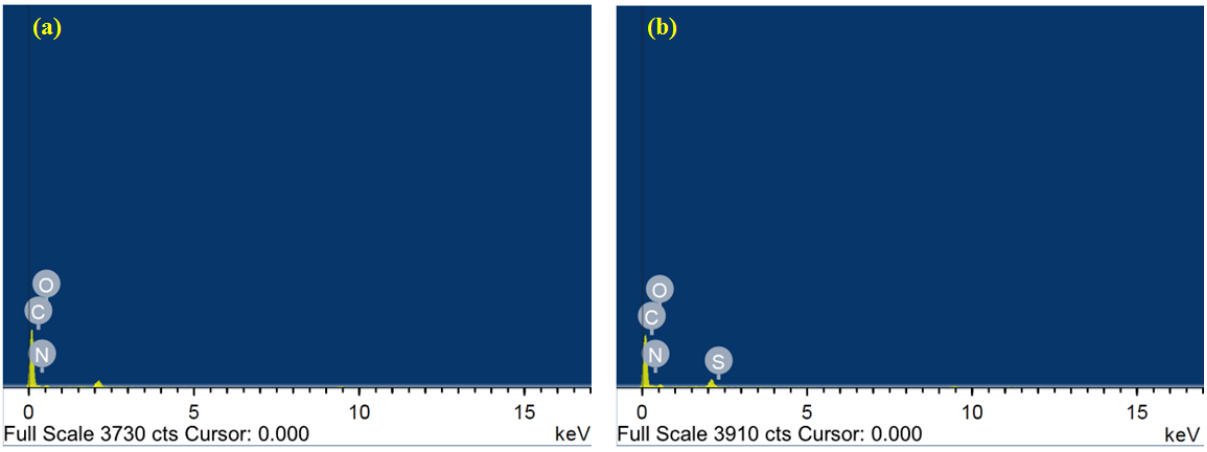

Fig. S2. EDAX elemental spectrum of crystals of (a) **Crystal-DMF**, and (b) **Crystal-DMSO**.

2. Crystallographic Data Collection and Refinement

Single Crystal X-ray Diffraction data were collected on a Bruker D8 Venture diffractometer equipped with Photon-III detector using monochromated Cu-Kα radiation (λ = 1.54178 Å) at 100 K using an Oxford cryostream low-temperature device for **Crystal-DMSO** and on a Bruker SMART APEX II CCD diffractometer using Mo-Kα radiation (λ = 0.71073 Å) at 276(2) K for **Crystal-DMF**. Unit cell measurement, data integration, scaling, and absorption corrections for the crystal were done with Bruker APEX II software.[1] Data reduction was carried out with Bruker SAINT suite.[2] Absorption correction was performed by multi-scan method implemented in SADABS.[3] Both the crystal structures were solved by direct methods using SIR 2014.[4] The crystal structure refinements with anisotropic non-hydrogen atoms

were done by full matrix least-squares calculations based on F^2 with SHELXL-2018/3[5], implemented in the OLEX2[6] program package. Hydrogen atoms of the hydroxyl and the NH group were located from a difference Fourier map, while other hydrogens were placed to their geometrically calculated positions and refined using a riding model with $U_{iso}(H) = 1.2U_{eq}(C)$ or $1.5U_{eq}(C\text{-}_{methyl})$. MERCURY[7] program was used for drawing the diagrams. *ORTEP* view of the asymmetric unit of **Crystal-DMSO** is shown in Fig. S3.

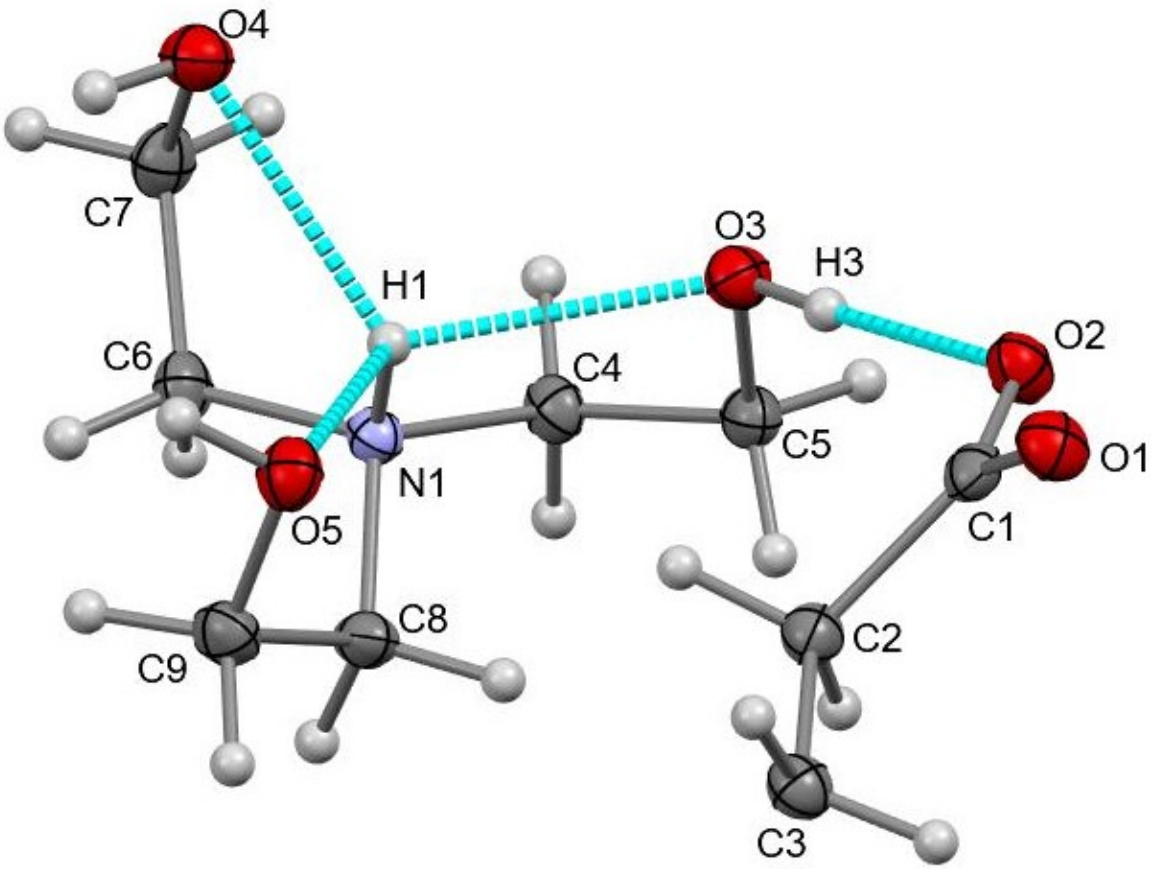

Fig. S3: *ORTEP* of **Crystal-DMSO** drawn at 50% ellipsoidal probability. The dotted lines represent intramolecular hydrogen bonds.

3. Diffraction Data of Crystal-DMSO and Crystal-DMF.

Table S1. Crystallographic data and refinement parameters for **Crystal-DMSO** and **Crystal-DMF**.

Crystal Code	**Crystal-DMSO**	**Crystal-DMF**
***CCDC No.**	2308950	2270635
Formula	$C_{18}H_{40}N_2O_{10}$	$C_{18}H_{40}N_2O_{10}$
Formula Weight	444.52	444.52
Crystal System	Monoclinic	Monoclinic
Space group	$P2_1/n$	$P2_1/n$
***a*[Å]**	5.3882(2)	5.4015(8)
***b*[Å]**	14.1701(4)	14.376(2)
***c*[Å]**	14.4214(4)	14.421(2)
α[°]	90	90
β[°]	95.4020(10)	94.264(7)
γ[°]	90	90
V[Å^3]	1096.20(6)	1116.7(3)
Solvent	DMSO	DMF
Z	2	2
***D*(calc) [g/cm^3]**	1.347	1.322
μ(MoKα) [mm^{-1}]	0.918	0.107
***F*(000)**	484	484
Crystal Size [mm^3]	0.066 × 0.053 × 0.051	0.32 × 0.3 × 0.3
Temperature (K)	100	296(2)
Radiation [Å]	CuKα (λ=1.54178)	MoKα (λ=0.71073)
θ (min, max) (°)	4.384, 79.941	2.833, 28.414
$h_{min,\ max}$, $k_{min,\ max}$, $l_{min,\ max}$	(-6,6); (-18, 18); (-18, 18)	(7, -7); (19, -19); (19, -19)

Treatment of Hydrogens	Mixed	Mixed
No. of unique/obs. reflections	2322/2079	2773/2405
No. of Parameters	152	149
R(int)	0.0641	0.0254
R_all, R_obs	0.0389, 0.0338	0.0525, 0.0465
wR2(all), wR2(obs)	0.0787, 0.0764	0.1437, 0.1375
$\Delta\rho_{min,\ max}$(eÅ^{-3})	-0.168/0.262	-0.224, 0.412
G.o.F	1.020	1.040

Table S2. Selected hydrogen bond parameters in **Crystal-DMSO**.

Donor-H···Acceptor	**D-H (Å)**	**H···A (Å)**	**D···A (Å)**	**D-H···A (°)**
Intra N1-H1···O3^{i}	0.92(14)	2.37	2.787(1)	108
Intra N1-H1···O4^{i}	0.92(14)	2.32	2.784(10	111
Intra N1-H1···O5^{i}	0.92(14)	2.30	2.779(1)	112
O3-H3···O2^{i}	0.85(18)	1.78	2.628(1)	177
C2-H2B···O5^{i}	0.99	2.76	3.715(1)	164
C2-H2A···O1^{ii}	0.99	2.51	3.489(1)	168
C5-H5A···O2^{ii}	0.99	2.69	3.336(1)	123
C5-H5A···O1^{ii}	0.99	2.80	3.776(1)	171
C4-H4B···O3^{ii}	0.99	2.34	3.332(1)	176
C8-H8B···O5^{ii}	0.99	2.50	3.458(1)	165
C6-H6B···O4^{ii}	0.99	2.51	3.415(1)	152
C4-H4A···O3^{iii}	0.99	2.48	3.430(1)	160
C5-H5B···O4^{iii}	0.99	2.64	3.550(1)	152
C7-H7A···O3^{iii}	0.99	2.77	3.640(1)	147

C7-H7A···O2^{iii}	0.99	2.93	3.798(1)	147
C3-H3A···O1^{iv}	0.99	2.99	3.835(1)	143
C9-H9A···O2^{v}	0.99	2.87	3.675(1)	139
O4-H4···O1 ^{vi}	0.88(18)	1.78	2.656(1)	170
C6-H6A···O1 ^{vi}	0.99	2.76	3.368(1)	120
O5-H5···O2 ^{vi}	0.90(18)	1.83	2.731(1)	174
O5-H5···O1^{vi}	0.90(18)	2.64	3.254(1)	126
C9-H9A···O1^{vi}	0.99	2.96	3.559(1)	120
C9-H9B···O4^{vii}	0.99	2.50	3.429(1)	156

Symmetry codes: *i*: x, y, z; ***ii*:** x+1, +y, +z; ***iii*:** -x+1, -y+1, -z+1; ***iv*:** -x, -y+1, -z+2

***v*:** -x+3/2, +y-1/2, -z+3/2; ***vi*:** -x+1/2, +y-1/2, -z+3/2; ***vii*:** x+1/2, -y+1/2, +z+1/2

4. Hirshfeld Surface Analysis.

Molecular Hirshfeld surfaces in crystal assemblies of **Crystal-DMSO** crystal is constructed by following the electron distribution premeditated as the sum of spherical atom electron densities. The Hirshfeld surface is distinctive for an individual crystalline architecture and a set of spherical atomic electron densities. The Hirshfeld surface portrays the probability of several intermolecular interactions in molecular crystals. The Hirshfeld surface of a molecule is established by points where the electron density of the molecule under concern is similar to the contribution from all other molecules. For every such point on that iso surface two distances are defined as d_e, the distance from the point to the nearest nucleus external to the surface, and d_i, the distance to the nearest nucleus internal to the surface. The normalized contact distance (d_{norm}), depending on d_e, d_i, and *vdW* radii of atom, shown in equation (S1), supports to detect the regions of specific significance to intermolecular interactions. The value of the d_{norm} is negative or positive when intermolecular contacts are shorter or longer than *vdW* separations, respectively. Due to the symmetry between d_e and d_i in the expression for d_{norm}, where two Hirshfeld surfaces connect, both will display a red spot identical in colour intensity along with size and shape.

$$d_{norm} = (d_i - r_i^{vdw})/ r_i^{vdw} + (d_e - r_e^{vdw})/ r_e^{vdw} \quad \text{(S1)}$$

where, r_i^{vdW} and r_e^{vdW} are the van der Waals radii of atoms.[8]

Molecular Hirshfeld surfaces and concomitant 2D-fingerprint plots were calculated and scrutinized using the program Crystal Explorer 3.1 For the purpose of this study all the Hirshfeld surfaces were generated using a standard (high) surface resolution. The fingerprint plots displayed each use the standard 0.4-2.6 Å view with the d_e and d_i distance scales displayed on the graph axes. The connectivity of de and d_i is expressed in the form a 2D fingerprint plot. 2D fingerprint plot offers the different intermolecular contacts within the crystal system. The Hirshfeld surfaces of **Crystal-DMSO** (Fig. 9a) have been mapped over d_{norm} (-1.1008 to 1.2174 Å), *shape index* (-0.9824 to 0.9953), *curvedness* (-4.0728 to 0.4478), d_e (0.6691 to 2.1431 Å) and d_i (0.6674 to 2.0874 Å). The surfaces are transparent for the understanding of the molecular architecture. The crystallographic information on different hydrogen-bonding patterns (Table S2) is expressed through these spots (Fig. 9a) where the deep red coloured large circular depressions of surfaces dictate the hydrogen-bonding contacts. H···H contacts are shown by other visible spots in the surfaces (Fig. 9a). The leading interactions between O···H (from deprotonated adipic acid and triethanolamine), and another O···H interaction (from deprotonated adipic acid and protonated triethanolamine) in **Crystal-DMSO** are given by the red coloured zones in the Hirshfeld surface (Fig. 9a). Different moderately weaker and longer contacts except hydrogen bonding patterns are expressed by small extent of area and light coloured on surfaces (Fig. 9a). H···H interactions are given as distinct spikes in the 2D fingerprint plot of **Crystal-DMSO** (Fig. S4). Complementary regions are given in the fingerprint plots where one molecule plays as donor ($d_e > d_i$) and the other acts as an acceptor ($d_e < d_i$). The fingerprint plots are separated to explore all significant close contacts between particular atom pairs. Other non-covalent intermolecular interactions like O···H/H···O, C···C, H···H, and C···H/H···C, appear as distinct spikes in 2D fingerprint plot (Fig. S4). These distinct spikes in 2D fingerprint plot (Fig. S4), combined in the full fingerprint (Fig. 9b), and conveys the impact of the contributions from different interactions towards the formation of **Crystal-DMSO** structure. The proportion of O···H, H···O, C···C, H···H, C···H, and H···C interactions are 20.1 %, 17.5 %, 1.1 %, 58.4 %, 1.6 %, and 1.3 %, of the Hirshfeld surfaces of **Crystal-DMSO**. The contributions of the various contacts, exhibited by **Crystal-DMSO**, have been illustrated in Fig. S4 which clearly shows the minimal effect of other interactions.

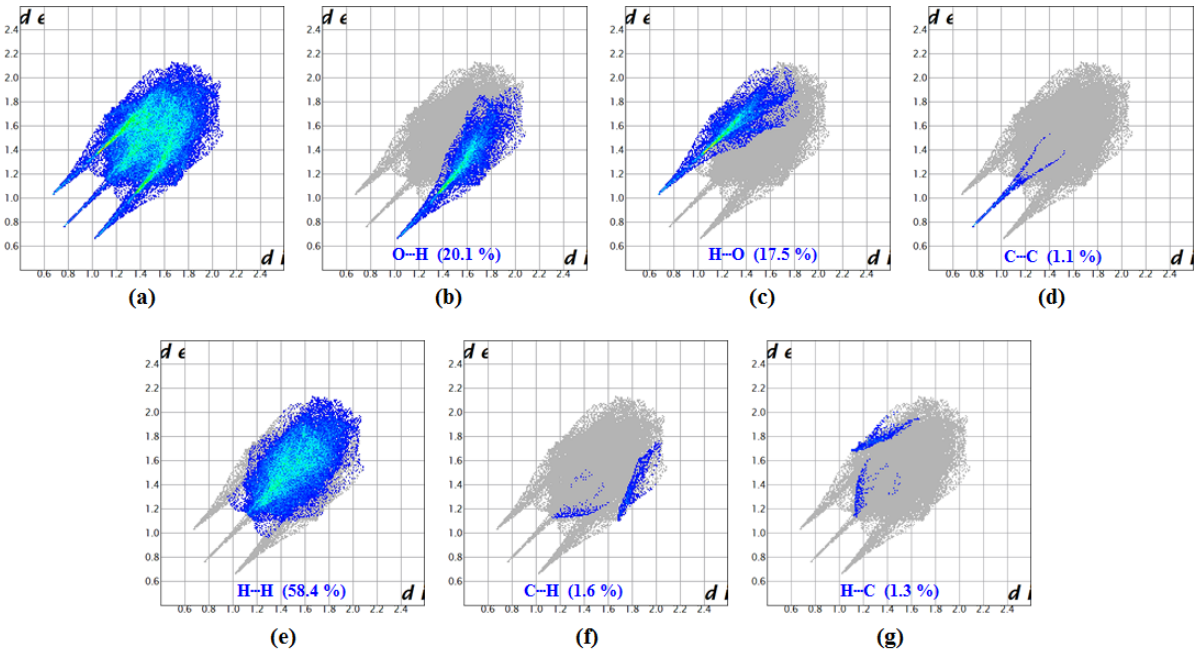

Fig. S4. Fingerprint plots of **Crystal-DMSO** corresponding to O···H/H···O, C···C, H···H, and C···H/H···C contacts involved in the crystal structure.

5. ESI-Mass analyses of ADP-TEA-DMF and ADP-TEA-DMF-MeCN.

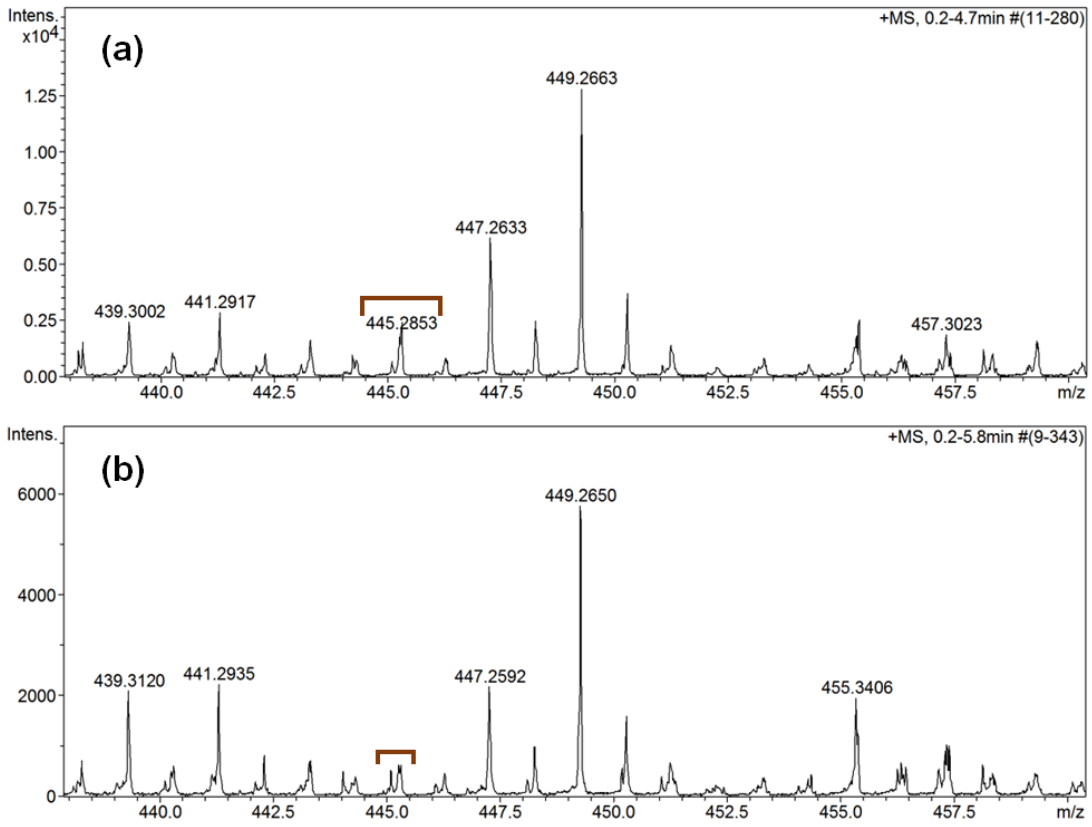

Fig. S5. ESI-Mass spectral data of (a) **ADP-TEA-DMF** organogel, and (b) **ADP-TEA-DMF-MeCN** organogel.

References:

(1) Bruker AXS, APEX2, version 2014.11-0, Inc. Madison, WI, **2014**.

(2) Bruker AXS, SAINT version 8.34 a, Inc. Madison, WI, **2013**.

(3) SADABS, version 2014/5, Inc. Madison, WI, 2014, **2014**.

(4) T. Gruene, H. W. Hahn, A. V. Luebben, F. Meilleur, G. M. Sheldrick, *J. Appl. Crystallogr*., 2014, **47**, 462–466.

(5) G. M. Sheldrick, *Acta Cryst*., 2015, **C71**, 3−8.

(6) O. V. Dolomanov, L. J. Bourhis, R. J. Gildea, J. A. K. Howard, H. Puschmann, *J. Appl. Cryst.,* 2009, **42**, 339−341.

(7) C. F. Macrae, I. Sovago, S. J. Cottrell, P. T. A. Galek, P. McCabe, E. Pidcock, M. Platings, G. P. Shields, J. S. Stevens, M. Towler, P. A. Wood, *J. Appl.Crystallogr*., 2020, **53**, 226–235.

(8) I. Feddaoui, Mohammed S. M. Abdelbaky, S. García-Granda, K. Essalah, C. Ben Nasr and M. L. Mrad, *J. Mol. Struct*., 2019, **1186**, 31-38.